ELSEVIER

Journal of Hydrology 228 (2000) 228–241

Journal of Hydrology

www.elsevier.com/locate/jhydrol

Influence of temporal variability of rainfall on interception loss. Part I. Point analysis

N. Zeng[a,b,*], J.W. Shuttleworth[c], J.H.C. Gash[d]

[a]*Department of Atmospheric Sciences, University of California, Los Angeles, CA 90095-1565, USA*
[b]*Institute of Geophysics and Planetary Physics, University of California, Los Angeles, CA 90095, USA*
[c]*Department of Hydrology and Water Resources, University of Arizona, AZ 85721, USA*
[d]*Institute of Hydrology, Wallingford, OX10 8BB, UK*

Received 14 June 1999; received in revised form 1 December 1999; accepted 16 December 1999

Abstract

An interception model that links the temporal variability of rainfall with the storm-based description of the interception process is derived. Analytical formulae for long-term interception loss are obtained for precipitation with statistical characteristics derived from observations.

The analysis of the results indicates that the point interception loss is controlled primarily by three time scales: the mean inter-storm arrival time τ_a, the mean storm duration τ_r and the time to evaporate a saturated canopy τ_0 which depends on canopy water holding capacity W_c and the wet canopy potential evaporation rate E_{l0}, and less importantly, on storm intensity. Additional assumption of rainfall stationarity leads to a relation between long-term interception loss and gross rainfall that requires a very small amount of input data.

The interception loss predicted by the analytical model agrees well with that of a Rutter model driven by a synthetic rainfall time series with the same statistics. Using the parameter values estimated from the observed rainfall data in the Amazon and southwestern France, the analytical results predict a long-term interception loss close to that observed.

Keywords: Rainfall interception; Analytical model; Rainfall temporal variability; Land–surface model

1. Introduction

The evaporation of intercepted rainfall by plant canopies typically accounts for 10–30% of the gross rainfall (Zinke, 1967; Blake, 1975). The unavailability of this fraction of rainfall to the soil modifies the surface–atmosphere energy and moisture balance. The layer of water on plant leaves also inhibits photosynthesis. Coupled land–atmosphere modeling has suggested potential climate sensitivities to the interception process (Scott et al., 1995).

The classic approaches to modeling interception loss use single-storm description and empirical relations between interception and gross rainfall (Horton, 1919; Zinke, 1967; Blake, 1975; Bras, 1990). Rutter et al. (1971) constructed a physically based numerical, point interception model. This model has been the basis of numerous subsequent analytical or semi-analytical models (Gash, 1979; Massman, 1983; Mulder, 1985; Whitehead and Kelliher, 1991; Liu, 1997). The Rutter model has also been implemented

* Corresponding author.
E-mail address: zeng@atmos.ucla.edu (N. Zeng).

0022-1694/00/$ - see front matter
PII: S0022-1694(00)00140-2

in many land–surface models, some of which have modifications to take account of the spatial variability of rainfall when applied to model grid boxes (e.g. Shuttleworth, 1988a; Entekhabi and Eagleson, 1989; Dickinson et al., 1993; Sellers et al., 1996).

While recognizing the importance of the temporal variability of rainfall on interception loss, early analytical models involved arbitrary assumptions about rainfall temporal characteristics. They generally assume regular rainfall events such as one or several uniformly distributed storms per day. Time averages of quantities are sometimes used and multiplied together. Because the temporal rainfall distribution is skewed and highly non-uniform, and because the interception process is highly non-linear, there is a large sensitivity to the precipitation regime assumptions (e.g. Lloyd, 1990), and adjusting factors are sometimes used (e.g. Pearce and Rowe, 1981).

One important characteristic of the interception process is that a typical storm can saturate the canopy very quickly because of its low water holding capacity. Therefore drizzles tend to produce more interception loss than intensive showers with the same total rainfall. On the other hand, how much of this intercepted water is evaporated after a storm depends on how soon the next storm comes. Thus various characteristics of the assumed precipitation regime can all have a large impact on the calculated interception loss. There is a strong need for clearly identifying the important characteristics.

Here we attempt an analytical model for point interception loss, taking into account of the stochastic rainfall distribution in time. The mathematical derivation would be more involved than some other theoretical models, but we expect to arrive at a solution that links the physically based, single-storm description of the interception process with long-term storm characteristics and gross rainfall. Follow-up work will address the sensitivities to assumptions about precipitation regimes and physical processes, and the model's application to global land–surface modeling. The derivation of the analytical model is described in Section 2. In Sections 3 and 4, the approximations and physical implications of the model are discussed. We then compare the model results with those of a Rutter model and observations. Conclusions are drawn in Section 5.

2. Analytical model

2.1. Interception loss during a storm/inter-storm event

2.1.1. Basic description of the interception process

Fig. 1 illustrates a conceptualized sequence of rainfall events and the corresponding time evolution in canopy water storage W and the evaporation of canopy interception E_{Ic}. Each rainfall event (including a storm period and an inter-storm period) is characterized by an intensity i, storm duration t_{r}, and inter-storm break period t_{b}. The storm inter-arrival time is defined as $t_{\mathrm{a}} \equiv t_{\mathrm{r}} + t_{\mathrm{b}}$. The storm intensity is assumed to be constant during a storm for mathematical convenience.

We adopt a version of the Rutter model for describing the canopy water storage and its evaporation. This type of model is suitable for describing point interception processes. In this context, a point is a plot or an area large enough to include the canopy and inter-canopy space while small enough such that the rainfall is homogeneous within this plot. Hence, caution needs to be taken if one applies this to a land–surface model as coupled to an atmospheric general circulation model (GCM) because convective rainfall is not homogeneous within a model grid box a few hundred kilometers wide.

A running water balance is maintained for the canopy storage:

$$\frac{\mathrm{d}W}{\mathrm{d}t} = P - E_{\mathrm{Ic}} - D_{\mathrm{r}} \tag{1}$$

where P is precipitation, E_{Ic} is canopy interception loss, and D_{r} is canopy drainage. Following Rutter, the evaporation of intercepted water E_{Ic} is:

$$E_{\mathrm{Ic}} = \frac{W}{W_{\mathrm{c}}} E_{\mathrm{I0}} \tag{2}$$

where E_{I0} is the potential rate of evaporation (wet canopy evaporation; Cain et al., 1998) which can be calculated using the Penman–Monteith equation by setting the canopy resistance to zero. E_{I0} needed here is during and shortly after the storms and will be assumed a constant during each individual model period (see below). A very useful time scale is the time it takes to evaporate a saturated canopy at this potential rate:

$$\tau_0 \equiv W_{\mathrm{c}}/E_{\mathrm{I0}} \tag{3}$$

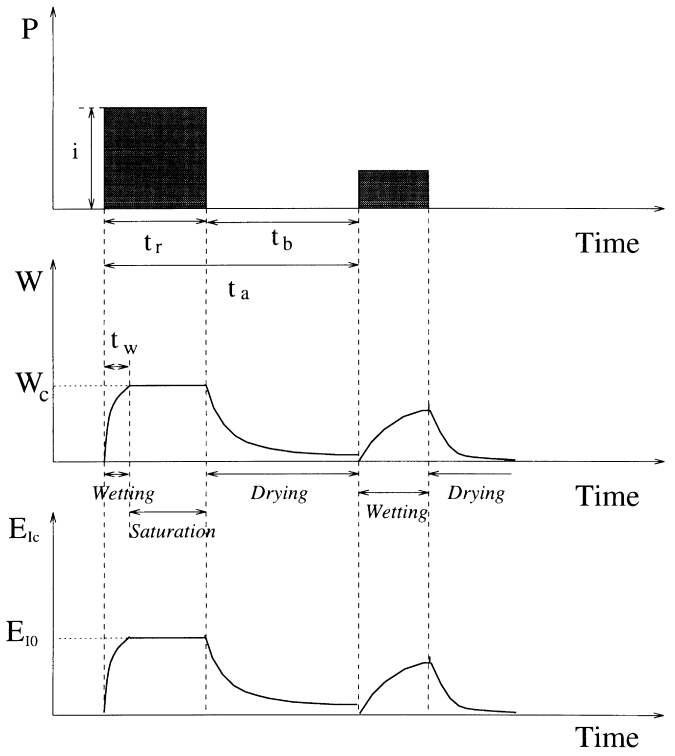

Fig. 1. Schematic diagram for two idealized rainfall events and the response in the canopy water storage W and the evaporation of the intercepted water E_{lc}. Each event is characterized by its intensity i, storm duration t_r and time for inter-storm break t_b, with the storm inter-arrival time $t_a \equiv t_r + t_b$. W_c is the saturation value for W, and E_{l0} is the wet canopy potential evaporation rate for the intercepted water. The second event corresponds to a case where the canopy is never saturated during the event. The analytical work assumes that all events start from a dry canopy and this neglects a second-order term. See text for discussion.

The drainage is taken as:

$$D_r = \begin{cases} \infty & W > W_c \\ 0 & W \le W_c \end{cases} \tag{4}$$

The water storage is thus not allowed to exceed a saturation value or capacity W_c, i.e. excess water is drained instantaneously. This is equivalent to choosing an infinite drainage coefficient in Rutter's exponential formulation. No drainage is allowed when the canopy is unsaturated. This version of the Rutter model will be referred to as Rutter2, while the version used by Shuttleworth (1988b) will be referred to as Rutter1. They differ somewhat in the D_r parameterization. Moreover, we assume a closed canopy here and then consider sparse canopy in Section 2.3.

As it rains over an initially dry canopy, the canopy water storage undergoes three stages: wetting, saturation and drying, as illustrated by the first storm event in Fig. 1. However, if the storm intensity is too weak or the duration is too short the canopy does not reach saturation before the storm ends, so it undergoes only two stages: wetting and drying, as shown for the second event in Fig. 1.

For the wetting period $(0, t_w)$, $D_r = 0$, and Eq. (1) becomes:

$$\frac{dW}{dt} = i - \frac{W}{\tau_0} \tag{5}$$

with solution:

$$W = i\tau_0(1 - e^{-t/\tau_0}) \tag{6}$$

If i is too small or the storm duration t_r is too short, the canopy will not be saturated (the second event in Fig. 1). The threshold rainfall intensity, i_s, when the canopy saturates just as the storm ends is determined

by the condition:

$$W_c = i_s \tau_0 (1 - e^{-t_r/\tau_0}) \tag{7}$$

This can be solved to yield:

$$i_s = E_{I0}(1 - e^{-t_r/\tau_0})^{-1} \tag{8}$$

As the canopy dries after rainfall has ceased:

$$\frac{dW}{dt} = -\frac{W}{\tau_0} \tag{9}$$

with solution:

$$W = W_r e^{-(t-t_r)/\tau_0} \tag{10}$$

where W_r is canopy water storage at the time the storm stops ($t = t_r$), which is W_c for the saturation case. For the unsaturated case Eq. (6) gives:

$$W_r = i\tau_0(1 - e^{-t_r/\tau_0}) \tag{11}$$

We now seek an analytical representation of the cumulative interception loss within an event. For the saturated case, our derivation is similar to the analytical model of Gash (1979), and for the unsaturated case it is similar to that of Mulder (1985) and others.

2.1.2. Events with saturated canopy

For events with $i > i_s$, the time to reach saturation t_w is given by:

$$W_c = i\tau_0(1 - e^{-t_w/\tau_0}) \tag{12}$$

Solving for t_w:

$$t_w = -\tau_0 \ln(1 - E_{I0}/i) \tag{13}$$

The cumulative interception loss normalized by E_{I0} during (0, t_w) is:

$$\begin{aligned}\int_0^{t_w} \frac{E_{Ic}}{E_{I0}} dt &= \frac{i}{E_{I0}} \int_0^{t_w} (1 - e^{-t/\tau_0}) dt \\ &= \frac{i}{E_{I0}} t_w - \frac{i}{E_{I0}} \tau_0 (1 - e^{-t_w/\tau_0}) \\ &= \frac{i}{E_{I0}} t_w - \frac{W_c}{E_{I0}}\end{aligned} \tag{14}$$

For the saturation period (t_w, t_r):

$$\int_{t_w}^{t_r} \frac{E_{Ic}}{E_{I0}} dt = t_r - t_w \tag{15}$$

For the drying period (t_r, t_a):

$$\int_{t_r}^{t_a} \frac{E_{Ic}}{E_{I0}} dt = \int_0^{t_b} e^{-t/\tau_0}\, dt = \tau_0(1 - e^{-t_b/\tau_0}) \tag{16}$$

Combining Eqs. (14)–(16) and substituting for t_w from Eq. (13), the normalized cumulative interception loss over the whole event period (0, t_a) is:

$$\begin{aligned}G_s \equiv \int_0^{t_a} \frac{E_{Ic}}{E_{I0}} dt = \tau_0(1 - i/E_{I0}) \ln(1 - E_{I0}/i) \\ + t_r - \tau_0\, e^{-t_b/\tau_0}\end{aligned} \tag{17}$$

2.1.3. Events with unsaturated canopy

For events with $i \le i_s$, one can find the cumulative interception loss for the wetting period (0, t_r) in a way similar to the saturation case:

$$\int_0^{t_r} \frac{E_{Ic}}{E_{I0}} dt = \frac{i}{E_{I0}} t_r - \frac{W_r}{E_{I0}} \tag{18}$$

For the drying period (t_r, t_a):

$$\int_{t_r}^{t_a} \frac{E_{Ic}}{E_{I0}} dt = \frac{W_r}{E_{I0}}(1 - e^{-t_b/\tau_0}) \tag{19}$$

Combining the above two equations and substituting W_r from Eq. (11), the normalized cumulative interception loss over the whole event period (0, t_a) is:

$$G_u \equiv \int_0^{t_a} \frac{E_{Ic}}{E_{I0}} dt = \frac{i}{E_{I0}} \{t_r - \tau_0(1 - e^{-t_r/\tau_0})\, e^{-t_b/\tau_0}\} \tag{20}$$

To summarize, the cumulative interception loss during a storm/inter-storm event over the period (0, t_a) can be expressed as:

$$G(i, t_r, t_b) \equiv \int_0^{t_a} \frac{E_{Ic}}{E_{I0}} dt = \begin{cases} G_s & i > i_s \\ G_u & i \le i_s \end{cases} \tag{21}$$

where the expressions for G_s, G_u and i_s are given in Eqs. (17), (20) and (8), respectively.

2.2. Interception loss driven by stochastic rainfall

The distribution of point rainfall is popularly modeled by gamma (including exponential) or log-normal distributions. We have analyzed the measured point precipitation from the Amazon Region Micrometeorology Experiment (ARME, Shuttleworth, 1988b). The

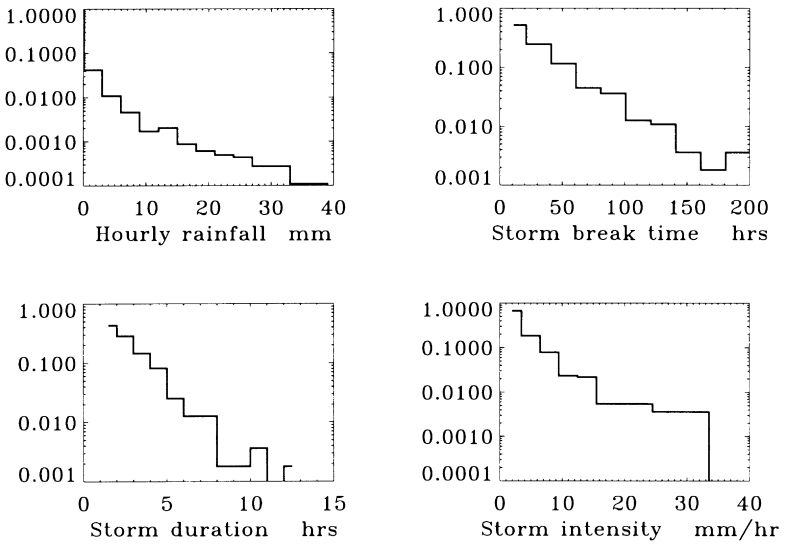

Fig. 2. Statistics of 25 month rainfall time series measured at central Amazon from the ARME experiment. Shown are normalized probability distributions of (a) hourly rainfall in mm h^{-1}; (b) inter-storm break time t_b in hours; (c) storm duration t_r in hours; and (d) storm intensity i in mm h^{-1}. A small number of extreme events give rise to a small probability off scale in the plot.

hourly rainfall data are available from September 1983 to September 1985 for a period of 25 months.

Fig. 2 shows the distribution of hourly rainfall intensity P, storm intensity i, storm duration t_r and storm break t_b from the 25 month ARME data. In identifying a storm event, a threshold of 0.25 mm is applied to remove the likely small artificial rainfall events due to single tip of the rain gauge bucket, following Lloyd (1990). On the log scale, the distributions appear very close to straight lines except for some extremely strong events that are undersampled because they have a small probability of occurring. This indicates that an exponential distribution is a good approximation. Similar results were found for mid-latitude sites by us (see below) and by others (e.g. Eagleson, 1978). We therefore assume exponential distributions for storm intensity i, storm duration t_r and inter-storm break time t_b respectively as:

$$f_i(i) = i_m^{-1}\, e^{-i/i_m} \tag{22}$$

$$f_r(t_r) = \tau_r^{-1}\, e^{-t_r/\tau_r} \tag{23}$$

$$f_b(t_b) = \tau_b^{-1}\, e^{-t_b/\tau_b} \tag{24}$$

where i_m, τ_r and τ_b are the means (expectation values) of i, t_r and t_b, respectively.

To maintain analytical tractability, we assume these distributions are independent of each other. The wet canopy potential evaporation rate for interception loss E_{I0} is assumed constant, and each event is assumed to start from a totally dry canopy. The latter slightly underestimates the interception loss because a typical storm quickly saturates the canopy anyway (a second-order term; see next section). Note that we do take account of the fact that the exponential tail after the next event is not evaporated, unlike Gash (1979) who assumed total evaporation of the canopy water before the next storm comes. Nevertheless, as we will show later, this amounts to only a small difference because $\tau_b \gg \tau_0$ (a first-order term; see next section). These subtleties are illustrated in Fig. 1 at the end of the first event and in the beginning of the second event.

For a sufficiently long period of time when enough independent events can be realized, the expectation value of the normalized cumulative interception loss for an event is:

$$[G] = \int_0^\infty \int_0^\infty \int_0^\infty G(i, t_r, t_b) f_i\, f_r\, f_b\, di\, dt_r\, dt_b \tag{25}$$

where [ ] denotes expectation value or mean, and the kernel function $G(i, t_r, t_b)$ is defined in Eq. (21).

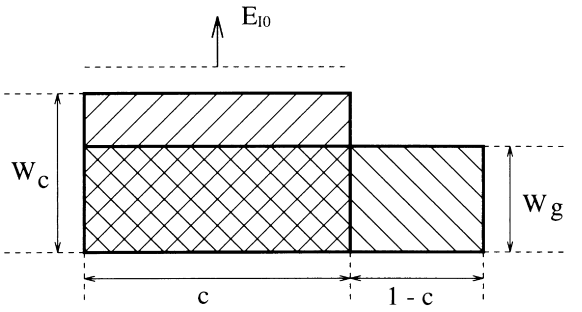

Fig. 3. Illustration of the relation between water storage capacity per canopy area W_c and water storage capacity per ground area W_g when canopy is not fully closed, with c being the fraction of vegetation cover. Evaporation of intercepted water occurs only over the vegetated area when saturated.

Integrating the above (see Appendix A) we obtain:

$$[G] = \alpha_1 \tau_r + \tau_0 \{\alpha_2 (1 + \epsilon_2)^{-1} - \alpha_3\} \quad (26)$$

where

$$\epsilon_1 \equiv E_{I0}/i_m \quad (27)$$

$$\epsilon_2 \equiv \tau_0/\tau_b \quad (28)$$

$$\delta \equiv \tau_r/\tau_0 \quad (29)$$

$$\alpha_1 = 1 - \frac{\epsilon_1}{\delta} + \frac{\alpha_3}{\delta^2} \quad (30)$$

$$\alpha_2 = 1 - \frac{2\alpha_3}{\delta} \quad (31)$$

$$\alpha_3 = \frac{\epsilon_1}{2} \ln \frac{\delta}{\epsilon_1} \quad (32)$$

$$\beta = \alpha_2 (1 + \epsilon_2)^{-1} - \alpha_3 \quad (33)$$

The integral involves Bessel functions of the second kind and approximations were made to neglect $\epsilon_1 \epsilon_2$ terms (second-order, see below; we use ϵ to denote a quantity much smaller than 1, while the other symbols can be of any order).

The expectation value of the event duration t_a is

$$\tau_a \equiv [t_a] = [t_r] + [t_b] = \tau_r + \tau_b \quad (34)$$

By definition, the average interception loss for a long period of time is just the cumulative value divided by the total time:

$$F \equiv \frac{\bar{E}_{Ic}}{E_{I0}} = \left[\int_0^{t_a} \frac{E_{Ic}}{E_{I0}} dt\right] \Big/ [t_a]$$

$$= \alpha_1 \frac{\tau_r}{\tau_a} + \frac{\tau_0}{\tau_a} \{\alpha_2 (1 + \epsilon_2)^{-1} - \alpha_3\} \quad (35)$$

where a bar denotes long-term mean values. We term F the interception function. It is the long-term average rate of interception loss $\bar{E}_{Ic}$ normalized by the potential rate E_{I0}. The coefficients α_1–α_3, ϵ_1, ϵ_2 and δ are related to the mean storm characteristics and environmental condition.

2.3. Interception loss for sparse canopies

For non-closed canopy, we consider the evaporation of intercepted rain only from the area covered by vegetation. Distinctions are made between the canopy water storage capacity per unit canopy area W_c discussed above, the canopy water storage capacity per ground area W_g and the canopy water holding capacity per leaf area W_0, as illustrated in Fig. 3. They are related to each other as:

$$W_g = W_0 L_{AI} \quad (36)$$

$$W_c = W_g/c \quad (37)$$

where L_{AI} is the leaf area index (leaf area per unit ground area) and c is the fraction of vegetation cover, so W_c is typically larger than W_g.

Eq. (35) returns the interception loss per canopy area E_{Ic}. In practice, however, what is commonly needed is the evaporation rate per unit ground area, E_I, which can be calculated using Eq. (35) as:

$$\bar{E}_I = c\bar{E}_{Ic} = cFE_{I0} \quad (38)$$

The factor c scales the evaporation rate from per unit canopy area to per unit ground area. The underlying assumption is that canopy evaporation is a purely vertical process so that horizontal mixing can be neglected. Therefore, canopy evaporation rate is given by evaporation rate per unit ground area E_{I0}. Eq. (38) is basically a weighted mean of the vegetated area and non-vegetated area, with the evaporation from bare soil neglected. This method can be generalized straightforwardly to multiple non-overlapping vegetation covers. Gash et al. (1995) and Valente et al. (1997) found that a similar procedure

Table 1
Parameter values for the Amazon site from 25 month ARME data

Parameter	Symbol	Value
Mean storm inter-arrival time	τ_a	30.3 h
Mean storm duration	τ_r	2.1 h
Mean storm intensity	i_m	3.8 mm h^{-1}
Canopy storage capacity	W_c	0.8 mm
Wet canopy evaporation	E_{I0}	0.21 mm h^{-1}
Vegetation cover	c	0.92

significantly improved their estimation of evaporation from sparse forests. In the following sections, this procedure is applied to both the analytical model and the Rutter model.

3. Approximations of the interception function and test against a Rutter model with synthetic forcing

As shown by Eq. (35), the interception function F is mostly determined by the three time scales: the storm inter-arrival time τ_a, the storm duration τ_r (the inter-storm break $\tau_b = \tau_a - \tau_r$) and the time to evaporate a saturated canopy at potential rate τ_0. Less important is the storm intensity i_m. This is because the canopy water storage capacity W_c is small so that most storms can fill it up in a short amount of time relative to the storm duration.

Using the 25 month ARME rainfall data we derived these parameter values, shown in Table 1. The canopy and evaporation parameters are from Shuttleworth (1988b) and Lloyd et al. (1988). Parameter values relevant to the analytical model are derived from these and shown in Table 2.

Table 2
Derived parameters for the Amazon

Parameter	Symbol	Value
W_c/E_{I0}	τ_0	3.8 h
E_{I0}/i_m	ϵ_1	0.06
τ_0/τ_b	ϵ_2	0.14
τ_r/τ_0	δ	0.56
Eq. (30)	α_1	1.10
Eq. (31)	α_2	0.77
Eq. (32)	α_3	0.07
Eq. (A9)	α_4	0.11
Eq. (33)	β	0.60

Among these, $\epsilon_1 \equiv E_{I0}/i_m \ll 1$ since the typical storm intensity is much larger than the evaporation rate. We also have $\epsilon_2 \equiv \tau_0/\tau_b \ll 1$, as the storms are so far separated such that the canopy has sufficient time to dry out, an assumption used by Gash (1979). Nevertheless, this effect adds a first-order correction (we consider the two terms outside the brackets in Eq. (35), namely τ_r/τ_a and τ_0/τ_a as zero-order for interception, although interception loss itself can be a higher-order quantity compared to E_{I0} or precipitation).

The first approximation we make is to assume the coefficients α_1 and β are site-independent constants (but not necessarily one); so we can rewrite Eq. (35) as:

$$F_1 = \alpha_1 \frac{\tau_r}{\tau_a} + \beta \frac{\tau_0}{\tau_a} \tag{39}$$

This approximation significantly reduces the input data needed and its application will be discussed in a later work. We have already neglected the second-order terms $O(\epsilon_1\epsilon_2)$ in deriving Eq. (35). A further approximation is to neglect all the first-order terms with respect to $\epsilon_1[O(\epsilon_1)]$, namely, $\alpha_1 \approx 1$, $\alpha_2 \approx 1$ and $\alpha_3 \approx 0$:

$$F_2 = \frac{\tau_r}{\tau_a} + \frac{\tau_0}{\tau_a}(1+\epsilon_2)^{-1} \tag{40}$$

The physical meaning of this approximation is that the storms are strong enough so that the canopy gets saturated instantaneously. The storm intensity-dependent terms ϵ_1 and $\alpha_1 - \alpha_3$ appear only in F so they add first-order corrections to F_2.

Finally, we approximate F_2 by dropping the first-order terms with respect to ϵ_2:

$$F_3 = \frac{\tau_r}{\tau_a} + \frac{\tau_0}{\tau_a} \tag{41}$$

In this approximation, the inter-storm break is long enough so that all the water is evaporated before the next storm comes. The difference between F_2 and F_3 indicates the error resulting from the assumption of total canopy dryout after a storm. F_3 corresponds to a very simple physical picture in which the evaporation is at its potential rate during a storm, and the saturated water is all evaporated after the storm. A similar form has been commonly used by hydrologists (e.g. Horton, 1919; Bras, 1990) though only to describe a single storm. Here we have shown that to first-order

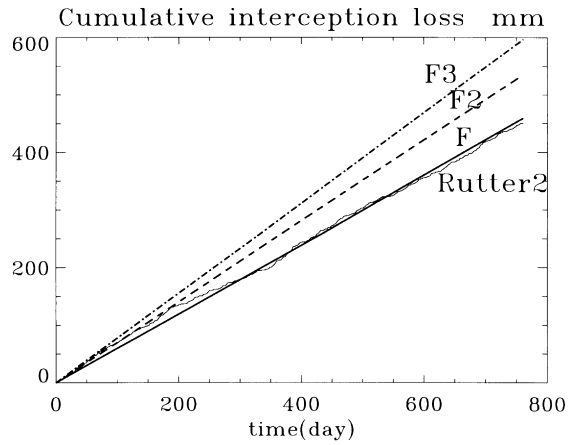

Fig. 4. Accumulated interception loss over a 760 day period as predicted by the analytical model and a Rutter model described in Section 2.1 (Rutter2; thin solid line) with the same underlying physics, but driven by a synthetic rainfall time series with the same statistics. F denotes the results from analytical interception function applied at each time step (thick solid line), while F_2 (dashed line) and F_3 (dash-dotted line) are two approximations of it. See text for more detail.

approximation (retain only zeroth-order terms), the single-storm description can be replaced by its mean characteristics and applied to long-term interception loss. The unapproximated analytical result Eq. (35) adds the corrections (complications) when taking into account the effects of finite storm intensity and incomplete drying of the canopy.

In order to test the accuracy of the analytical results and the successive approximations made for the interception function F, we run the numerical Rutter2 model described in the beginning of Section 2.1. A synthetic rainfall time series is generated as a Monte Carlo realization of the exponential distributions (22)–(24) using the ARME parameters for i_m, τ_b and τ_r (Table 1). The model was run at 1 min time step using the ARME parameters. Fig. 4 shows the cumulative interception loss from the Rutter model and the approximations F, F_2 and F_3. The results from the interception functions are straight lines because they are constant in time, corresponding to a stationary rainfall process. As expected, F is very close to the Rutter2 model (F_1 is identical to F in this case), while F_2 and F_3 overestimate interception loss by about 17% and 30%, respectively. Theoretically speaking, the difference between F and the Rutter2 model comes only from the approximations made in the integration of Eq. (21) and the randomness of the rainfall time series, because the underlying physics is the same.

4. Test of the model against observations

In the real world, the exponential distributions and the independence assumption are not exactly satisfied. This is especially true for extreme events. Observational limitation adds a further complication. For instance, the typical resolution of 1 h in rainfall observation undoubtedly leads to overestimation of the storm duration τ_r which is typically 2 h. Despite these complications, we expect that the theory can capture the first-order effects, thus providing a reasonable estimation in the face of many other uncertainties.

Eq. (35) is best applied to a very long period so enough rainfall events are included. This is compromised by the fact that the real rainfall is not stationary in time. Notably it possesses seasonal variation. In sub-tropical regions, rainfall often has very different characteristics between the summer convective storm regime and winter large-scale precipitation regime. The best time scale for applying Eq. (35) is probably sub-seasonal scale. In the following, we will apply it at the monthly time scale, acknowledging that the calculated interception loss may not be sufficiently accurate for each month but expecting adjacent months to compensate for each other.

We have analyzed the observed rainfall characteristics over a dry season and a wet season separately using the ARME data and find that the mean storm duration τ_r and mean storm intensity i_m differ by less than 10% while the inter-arrival time τ_a differs by a factor of two, corresponding to a difference of a factor of two in precipitation. This indicates that the storm characteristics (τ_r and i_m) stay largely the same while the storm occurring frequency ($1/\tau_a$) changes from one climate regime to another. Theoretical considerations have been brought forth (e.g. Emanuel and Bister, 1996) to explain this tendency. The atmospheric convection responds to an enhancement in thermal forcing by more frequent occurrence (rather than more vigorous convective events) to remove the instability, while the characteristics are determined by other factors (however, see Section 5 for large-scale

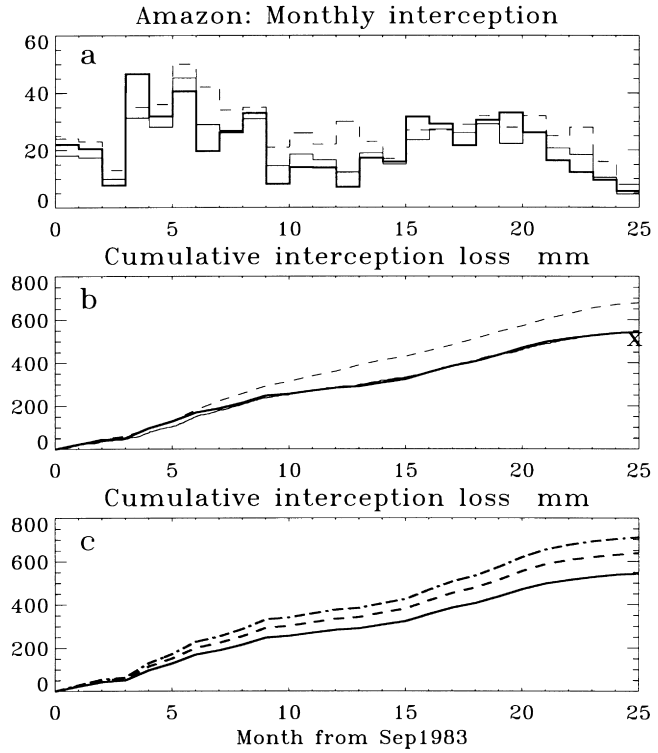

Fig. 5. (a) Monthly mean; and (b) cumulative interception loss predicted by the analytical interception function F (thick solid line) and simulated by the Rutter model (Rutter2, thin solid line). (c) Cumulative interception loss predicted by the analytical interception function F (solid line; as in b), F_2 (dashed), F_3 (dash-dotted). Also plotted are the results from the Rutter model of Shuttleworth (1988b); dashed line), and the measured total interception loss (Lloyd et al. 1988; scaled to the whole period using the 625 day available data, marked by a cross X on the right).

precipitation). Although it is straightforward to calculate τ_r and i_m for each month, we will simply take the mean values from the 25 month data here and use the same values for each month. The results are found to be insensitive to this difference. The main appeal of this approach is that the resulting simplifications require less input data. Thus, our task here is simply to find τ_a for each month which is related to the monthly mean precipitation $\bar{P}$ by:

$$\bar{P} = \frac{[it_r]}{[t_a]} = \frac{i_m \tau_r}{\tau_a} \tag{42}$$

Substituting τ_a with $\bar{P}$, one can then implement the interception functions F, F_1, F_2 and F_3 as:

$$F = \frac{\bar{P}}{i_m}\left\{\alpha_1 + \frac{\tau_0}{\tau_r}\left[\alpha_2\left(1 + \frac{\tau_0}{\tau_b}\right)^{-1} - \alpha_3\right]\right\} \tag{43}$$

$$F_1 = \frac{\bar{P}}{i_m}\left\{\alpha_1 + \beta\frac{\tau_0}{\tau_r}\right\} \tag{44}$$

$$F_2 = \frac{\bar{P}}{i_m}\left\{1 + \frac{\tau_0}{\tau_r}\left(1 + \frac{\tau_0}{\tau_b}\right)^{-1}\right\} \tag{45}$$

$$F_3 = \frac{\bar{P}}{i_m}\left\{1 + \frac{\tau_0}{\tau_r}\right\} \tag{46}$$

where $\bar{P}$ is the monthly mean rainfall, and τ_b is calculated using $\tau_b = \tau_a - \tau_r$. Note that all the other parameters except for $\bar{P}$ and τ_b are constant for the whole 25 month period.

The predicted monthly and cumulative interception loss using Eqs. (43) and (38) are shown in Fig. 5, as well as the Rutter2 model described in Section 2.1 driven by the observed ARME hourly rainfall data running at 1 min time step. For comparison, also plotted is the measured total interception loss from

Table 3
Parameter values for Les Landes from 11 month data

Parameter	Symbol	Value
Mean storm inter-arrival time	τ_a	33.2 h
Mean storm duration	τ_r	2.5 h
Mean storm intensity	i_m	1.0 mm h^{-1}
Canopy storage capacity	W_c	0.56 mm
Wet canopy evaporation	E_{I0}	0.17 mm h^{-1}
Vegetation cover	c	0.45

Table 4
Derived parameters for Les Landes

Parameter	Symbol	Value
W_c/E_{I0}	τ_0	3.3 h
E_{I0}/i_m	ϵ_1	0.16
τ_0/τ_b	ϵ_2	0.11
τ_r/τ_0	δ	0.77
Eq. (30)	α_1	1.10
Eq. (31)	α_2	0.67
Eq. (32)	α_3	0.12
Eq. (A9)	α_4	0.16
Eq. (33)	β	0.48

the ARME experiment (Lloyd et al., 1988; scaled to the whole period using the data from 625 days of available data), and the results from the Rutter1 model used by Shuttleworth (1988b). Their version of the Rutter model differs from ours in that theirs allows supersaturation. This tends to predict more interception loss than Rutter2. The difference in the results partly comes from the fact that we used constant parameter values throughout the 25 months while their parameters change with time. It is interesting to note that the interception function F_2 and F_3 overestimate by amounts similar to the Rutter1 model.

Fig. 5 shows that the theoretical interception function gives very similar results to Rutter2 in the cumulative loss, while the month by month values differ somewhat. The totals at the end of the 25 months from the interception function F and Rutter2 are similar, at about 543 mm, while the measured value is 521 mm. The total for Rutter1 is 680 mm.

It is interesting to see the effects of calculating the total interception loss using τ_a derived for the whole period (Table 1) rather than monthly. This involves a single calculation using Eqs. (35) and (38). The result gives a total interception loss of 537 mm, very close the total calculated from the monthly data. This is no surprise in the sense that the sampling is better for a longer period. This also indicates that regime transition from season to season is probably not important in the Amazon, where the rainfall is almost always convective.

Similar tests are conducted for a mid-latitude site in Les Landes forest in southwestern France during the Hydrological Atmospheric Pilot Experiment (HAPEX, Gash et al. 1995). The parameter values are listed in Tables 3 and 4. The monthly and cumulative interception loss calculated by the model and the Rutter2 model are plotted in Fig. 6. The total interception loss over the 11 month period is 77 mm as calculated by the current model, 79 mm by the Rutter2 model and 73 mm measured by Gash et al. (1995). The analytical model F using Eqs. (35) and (38) and τ_a for the whole period (Table 3) gives a value of 81 mm.

Two things can be said about these results. The good agreement between the theory and Rutter2 driven by real data indicates that the theory is capable of predicting long-term interception loss using average rainfall characteristics, despite the simple (but more realistic than in early works) assumptions made about the rainfall statistics. Secondly, the measurement uncertainty for the observed total interception loss is about 200 mm at the ARME site (Lloyd et al. 1988) and the results from all the models above including Rutter1 fall in this error range. At a stage when research is still talking about the kind of accuracy with an error factor of two in land–surface models (e.g. Lloyd 1990; Koster and Milly 1997), the interception function approach proposed here (including the approximations F_2 and F_3 and fixed storm characteristics τ_r and i_m) offers a simple and powerful tool for estimating long-term interception loss (Zeng et al. 2000).

5. Discussion and conclusion

Traditionally, one type of simple model of interception is storm-based (Horton, 1919):

$$E_I = W_g + cE_{I0}t_r \tag{47}$$

Another type of model is empirically based (Horton,

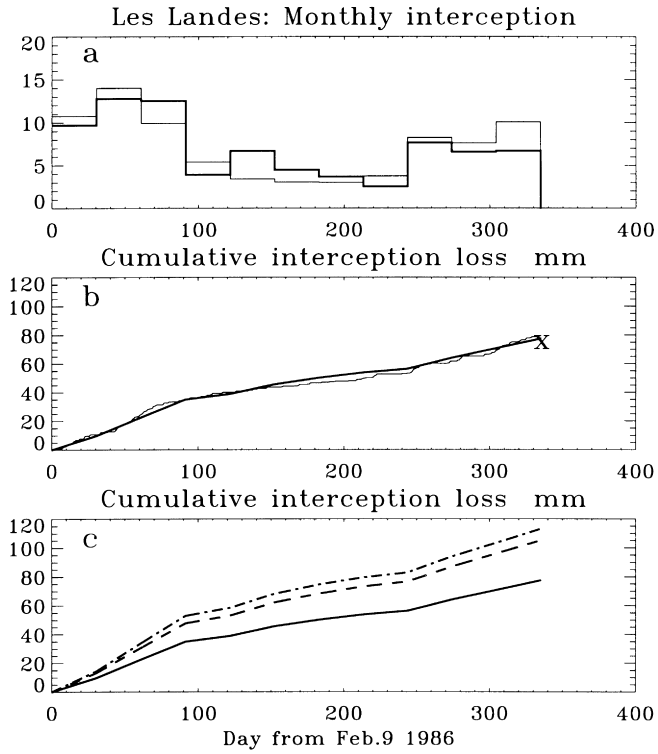

Fig. 6. (a) Monthly mean; and (b) cumulative interception loss for the Les Landes site in southwestern France predicted by the analytical interception function F (thick solid line) and simulated by the Rutter model (Rutter2, thin solid line). (c) Cumulative interception loss predicted by the analytical interception function F (solid line; as in b), F_2 (dashed), F_3 (dash-dotted). Also plotted is the measured total interception loss (Gash et al. 1995) marked by a cross X on the right.

1919; Zinke, 1967; Blake, 1975):

$$E_I = aP_G + b \tag{48}$$

where P_G is gross rainfall and a and b are empirically derived parameters. Eq. (48) has been used for both single-storm and long-term interception. In comparing Eqs. (47) and (48), Horton stated that: "For practical purposes, it will probably often be more convenient to utilize interception results or formulae expressed in terms of amount of precipitation rather than in terms of shower duration, although the latter method of expressing results appears to be more logical".

Comparing Eqs. (48) with (43)–(46), our analytical model provides a theoretical basis for the empirical linear relationship (quasi-linear in the theory) based on the storm description. The more realistic assumptions about temporal rainfall variability have allowed the inclusion of the effects of finite storm intensity and incomplete drying of the canopy. The physical processes and their relative importance are quantified by our analysis of successive approximations. The coefficients are estimated based on the physical processes including storm, canopy and environmental characteristics. Thus the analytical model here provides the link needed between the two apparently different approaches Horton pondered upon three-quarter of a century ago. In Eqs. (43)–(46), the equivalent of the intercept b in Eq. (48) is necessarily zero because our formulation applies to a long period of time, so there should be no intercepted water when there has been a long drought. The empirical formula (48) was sometimes applied to shorter periods when evaporation of remaining water from previous storm is included (Gash, 1979).

Extra effort in deriving the formulation returns rather simple results. The analysis indicates that long-term interception loss is controlled primarily by three time scales: the mean storm inter-arrival

time τ_a, the mean storm duration τ_r and the time to evaporate a wet canopy τ_0. The former two time scales are precipitation related while the latter depends on canopy water holding capacity and wet canopy evaporation rate. Also relevant but less important is storm intensity because most storms saturate the canopy quickly.

The seemingly direct proportionality of interception loss to E_{I0} in Eq. (38) actually only applies to the part related to storm duration τ_r (first term in Eq. (35)) because in the second term τ_0 includes E_{I0} (Eq. (3)). So they cancel out in the equation for E_I. This quantity is nonetheless important and requires care when one attempts to estimate it using limited amount of observation data. For instance, one would assume an upper limit for E_{I0} being the net radiation and it can be estimated using the Penman–Monteith equation applied to some kind of mean condition over the whole period. The observations in both validation sites show that E_{I0} tends to be somewhat larger than the long-term mean net radiation. This indicates that during and shortly after the storms, the canopy environmental condition is such that interception loss rate can temporarily exceed the available radiation, implying a negative sensible heat or a cooling of the surface (Stewart, 1977). It is not clear what causes the larger (about 25% in the Amazon case) evaporation rate than net radiation.

The theoretical results agree well with a Rutter model when driven by synthetic rainfall time series. The successive approximations reveal the relative importance of various physical characteristics and processes. Additional assumption about the stationarity of convective rainfall allows the model to be applied to realistic situations with gross rainfall as the major input variable. Tests against observations and a Rutter model in the Amazon and southwestern France demonstrate the theory's reasonable success in predicting monthly interception loss, and for the cumulative interception loss over longer periods they can agree better because the statistical assumptions are better satisfied.

It is worth noting that the analytical formulae can be applied to long-term total interception by a single calculation provided with the mean characteristics listed above. In a tropical convective rainfall environment, these characteristics appear to be largely invariant except for the storm inter-arrival time that can be directly linked to gross rainfall. This lends a potentially powerful method for a quick and reasonably accurate estimate of interception loss with minimum amount of input data. At mid-latitudes, however, storm characteristics can vary more significantly. For instance, the mean storm duration derived at Boston (Eagleson, 1978) is more than twice as long as at Les Landes. A Poisson process-based analysis indicates that mid-latitude storms tend to have varying storm depth much more than storm frequency (Salvucci and Song, 2000), in contrast to the convective storm characteristics in the Amazon data. While further analysis of the rainfall characteristics and tests of the present model at various locations are needed, the first order distinction one can make is probably between convective and large-scale precipitation regimes. This is especially relevant because many sub-tropical and mid-latitude locations tend to have convective storms in summer and large-scale rainfall in winter.

Many current land–surface models used in GCMs apply a Rutter model directly to a GCM grid box which is typically a few 100 km wide. Despite efforts in incorporating sub-grid rainfall variation, the lack of or arbitrary assumptions about the temporal correlation is probably responsible for the poor simulation of interception loss in the tropics (e.g. Lloyd, 1990; Fig. 3 of Koster and Milly 1997). Insights provided by the present analysis can help the treatment of interception loss in these models.

Acknowledgements

We acknowledge discussions with R. Koster, J.D. Neelin and Y.C. Sud, and comments from an anonymous reviewer. This research was supported by NSF grant ATM-9521389 and NOAA grant NA86GP0314 awarded to J.D. Neelin, and a grant from the NASA IPA program to NZ.

Appendix A

We first integrate Eq. (21) with respect to i:

$$\int_0^\infty Gf_i\,\mathrm{d}i = \int_{i_s}^\infty G_s f_i\,\mathrm{d}i + \int_0^{i_s} G_u f_i\,\mathrm{d}i$$

$$\approx \mathrm{e}^{-z}\{t_r + \tau_0(1-\mathrm{e}^{-t_b/\tau_0})\} + \tau_0\frac{\epsilon_1}{2}\ln z$$

$$+ \epsilon_1^{-1}\{1-(1+z)\mathrm{e}^{-z}\}\{t_r - \tau_0(1-\mathrm{e}^{-t_r/\tau_0})\mathrm{e}^{-t_b/\tau_0}\} \quad \text{(A1)}$$

where

$$\epsilon_1 \equiv E_{I0}/i_m \tag{A2}$$

$$z \equiv i_s/i_m = \epsilon_1(1 - e^{-t_r/\tau_0})^{-1} \tag{A3}$$

In integrating the above, the symbolic algebra software Mathematica (Wolfram, 1996) has been used. The mean storm intensity is much larger compared to the potential evaporation rate (see Section 2), i.e. $i_m \gg E_{I0}$, or $\epsilon_1 \ll 1$. This has been used in integrating the logarithmic term in Eq. (17) by neglecting $O(\epsilon_1^2)$ terms.

Now integrate the above with respect to t_r:

$$\int_0^\infty \left(\int_0^\infty G f_i \, di \right) f_r \, dt_r = \alpha_1 \tau_r + \tau_0 \{ \alpha_2 (1 - e^{-t_b/\tau_0}) - \alpha_3 - \alpha_4 e^{-t_b/\tau_0} \} \tag{A4}$$

where

$$\delta \equiv \tau_r/\tau_0 \tag{A5}$$

$$\alpha_1 = 1 - \frac{\epsilon_1}{\delta} + \frac{\alpha_3}{\delta^2} \tag{A6}$$

$$\alpha_2 = 1 - \frac{2\alpha_3}{\delta} \tag{A7}$$

$$\alpha_3 = \frac{\epsilon_1}{2} \ln \frac{\delta}{\epsilon_1} \tag{A8}$$

$$\alpha_4 = \frac{\alpha 3}{\delta} \tag{A9}$$

The integral involves Bessel functions of the second kind and approximations were made using $\epsilon_1 \ll 1$.

Integrate the above with respect to t_b:

$$\int_0^\infty \left(\int_0^\infty \left(\int_0^\infty G f_i \, di \right) f_r \, dt_r \right) f_b \, dt_b = \alpha_1 \tau_r + \tau_0 \{ \alpha_2 (1 + \tau_0/\tau_b)^{-1} - \alpha_4 (1 + \tau_b/\tau_0)^{-1} - \alpha_3 \} \tag{A10}$$

The second term in the brackets is a second-order term, i.e. it involves $\epsilon_1 \epsilon_2$ where $\epsilon_2 \equiv \tau_0/\tau_b \ll 1$, and it can be safely neglected to give Eq. (26) in Section 2.

References

Blake, G.J., 1975. The Interception Process. In: Chapman, T.G., Dunin, F.X. (Eds.). Prediction in Catchment Hydrology, Australian Academy of Science, Canberra, pp. 59–81.

Bras, R.L., 1990. Hydrology: an Introduction to Hydrologic Science, Addison-Wesley, Reading, MA (p. 643).

Cain, J.D., Batchelor, C.H., Gash, J.H.C., Harding, R.J., 1998. Hydrology and Earth System Sciences, European Geophysical Society (comment on the paper "Towards a rational definition of potential evaporation" by J.P. Lhomme).

Dickinson, R.E., Henderson-Sellers, A., Kennedy, P.J., 1993. Biosphere-Atmosphere Transfer Scheme (BATS) Version 1e as coupled to the NCAR Community Climate Model. NCAR Tech. Note NCAR/TN-387 + STR (Bourlder, CO; p. 72).

Eagleson, P.S., 1978. Climate, soil, and vegetation. 2. The distribution of annual precipitation derived from observed storm sequences. Water Resour. Res. 14, 713–721.

Emanuel, K.A., Bister, M., 1996. Moist convective velocity and buoyancy scales. J. Atmos. Sci. 53, 3276–3285.

Entekhabi, D., Eagleson, P.S., 1989. Land surface hydrology parameterization for atmospheric general circulation models including subgrid scale spatial variability. J. Climate 2, 816–831.

Gash, J.H.C., 1979. An analytical model of rainfall interception by forests. Q. J. R. Meteorol. Soc. 105, 43–55.

Gash, J.H.C., Lloyd, C.R., Lachaud, G., 1995. Estimating sparse forest rainfall interception with an analytical model. J. Hydrol. 170, 79–86.

Horton, R.E., 1919. Rainfall interception. Monthly Weather Rev. 47, 603–623.

Koster, R.D., Milly, P.C.D., 1997. The interplay between transpiration and runoff formulations in land surface schemes used with atmospheric models. J. Climate 10, 1578–1591.

Liu, S., 1997. A new model for the prediction of rainfall interception in forest canopies. Ecol. Model. 99, 151–159.

Lloyd, C.R., 1990. The temporal distribution of Amazonian rainfall and its implications for forest interception. J. R. Meteor. Soc. 116, 1487–1494.

Lloyd, C.R., Gash, J.H.C., Shuttleworth, W.J., Marques, A.O., 1988. The measurement and modelling of rainfall interception by Amazonian rainforest. Agric. For. Meteorol. 43, 277–294.

Massman, W.J., 1983. The derivation and validation of a new model for the interception of rainfall by forests. Agric. Meteorol. 28, 261–286.

Mulder, J.P.M., 1985. Simulating interception loss using standard meteorological data. In: Hutchison, B.A., Hicks, B.B. (Eds.). The Forest–Atmosphere Interaction, Reidel, Drodrecht, pp. 177–196.

Pearce, A.J., Rowe, L.K., 1981. Rainfall interception in a multistoried evergreen mixed forest: estimates using Gash's analytical model. J. Hydrol. 49, 341–353.

Rutter, A.J., Kershaw, K.A., Robins, P.C., Morton, A.J., 1971. A predictive model of rainfall interception in forests. I. Derivation of the model from observations in a plantation of corsican pine. Agric. Meteorol. 9, 267–384.

Salvucci, G.D., Song, C., 2000. Derived distributions of storm depth and frequency conditioned on monthly total precipitation:

adding value to historical and satellite-derived estimates of monthly precipitation. J. Hydrometerology, in press.

Scott, R., Koster, R.D., Entekhabi, D., Suarez, M.J., 1995. Effect of a canopy interception reservoir on hydrological persistence in a general circulation model. J. Climate 8, 1917–1922.

Sellers, P.J., et al., 1996. A revised land surface parameterization (SiB2) for atmospheric GCMs. Part I. Model formulation. J. Climate 9, 676–705.

Shuttleworth, W.J., 1988a. Macrohydrology—the new challenge for process hydrology. J. Hydrol. 100, 31–56.

Shuttleworth, W.J., 1988b. Evaporation from Amazonian rain forest. Proc. R. Soc. London Ser. B 233, 321–346.

Stewart, J.B., 1977. Evaporation from the wet canopy of a pine forest. Water Resour. Res. 13, 915–921.

Valente, F., David, J.S., Gash, J.H.C., 1997. Modelling interception loss for two sparse eucalypt and pine forests in central Portugal using reformulated Rutter and Gash analytical models. J. Hydrol. 190, 141–162.

Whitehead, D., Kelliher, F.M., 1991. A canopy water balance model for a Pinus radiata stand before and after thinning. Agric. For. Meteorol. 55, 109–126.

Wolfram, S., 1996. The Mathematica Book. 3rd ed., Wolfram Media, Inc. and Cambridge University Press, Cambridge (p. 1403).

Zeng, N., Neelin, J.D., Chou, C., 2000. The first quasi-equilibrium tropical circulation model-implementation and simulation. J. Atmos. Sci., in press.

Zinke, 1967. (Forest interception studies in the United States). In: Sopper, W.E., Lull, H.W. (Eds.). International symposium on Forest Hydrology, Pergamon Press, Oxford, pp. 137–161.